Erasmus Mundus Joint Master Degree in Nuclear Physics

Université Caen Normandie

Study of a new design of the VENUS-F reactor and its instrumentation for SALMON phase 2 Pulsed Neutron Source experiments

Master Thesis presented by

Guillermo Ortega-Ureta

Tutors

Jean-Luc Lecouey
Nathalie Marie-Nourry

Jean-Luc Lecouey
November 13th, 2023

France, July 2023

Acknowledgements

To all the great teachers that have kept my deep love for Physics alive.

To my tutors, for their patience, understanding and continuous support, specially to Jean-Luc, that has made the reckless decision of keeping me working with him three more years.

To all my friends back home in Spain, that help me be the best version of myself, that share my tears and my laughter, and that continuously remind me why life is worth living to the fullest.

To all the amazing new friends that I have made these past two years, that have shared this journey of discovery and given me the energy and the motivation to never give up, to always be excited about the next thing.

And to my family, my greatest support and the reason I am who I am today.

Contents

Chapter 1

Introduction

The production and usage of nuclear energy is an important topic to bear in mind in the context of an energetic transition towards reducing our carbon emissions and achieving a more sustainable society, besides playing a significant role in meeting the current global energy demands. France is particularly prominent in this subject, with nuclear power representing 40% of its primary energy production in 2020 [6]. The numerous advantages of this energy source include very low carbon emissions, high efficiency and reliability, as well as allowing for a consistent power supply. However, nuclear power production is the subject of numerous debates and is often harshly criticized by the general public, therefore it is crucial to recognize the challenges it still presents, two of the most prominent ones being the management of nuclear waste and specially the safety of nuclear power plants, the latter being the main motivation behind this work.

Nuclear safety is based on three main pillars: prevention, to minimize the probability of a problematic situation happening; monitoring, to swiftly detect any anomalies in the behavior of the reactor; and action, to ultimately correct said anomalies and return everything to normality. This study puts its focus on monitoring, and in particular on the surveillance of reactor fuel loading, one of the most delicate and error-prone operations that take place in a reactor. In these procedure, that takes place either yearly or every year and a half, all the fuel assemblies are first removed from the core in a precise order, and then a fraction of them, the most burned-up, are substituted by new ones. Finally, all of them are reinserted in the core, again in a particular order. An example of a loading pattern is shown in Figure 1.1. These orders are detailed in loading plans, which are carefully designed in advance in order to optimize fuel burn-up, but also to maintain the core under the appropriate conditions to guarantee safety at all times. If a mistake is made and the loading plan is not properly followed, incidents of even serious accidents could ensue.

On April 2^{nd}, 2001, at the Dampierre-en-Burly nuclear power plant, assembly number 25 was forgotten in its storage during a core reloading. This caused all the subsequent assemblies to be loaded one position too early, and this mistake was not discovered until 114 more assemblies had been wrongly loaded, thus significantly reducing the security margin from criticality that was established for a safe usage of the reactor [18].

This incident ended up being categorized as level 2 on the INES scale [7], and even

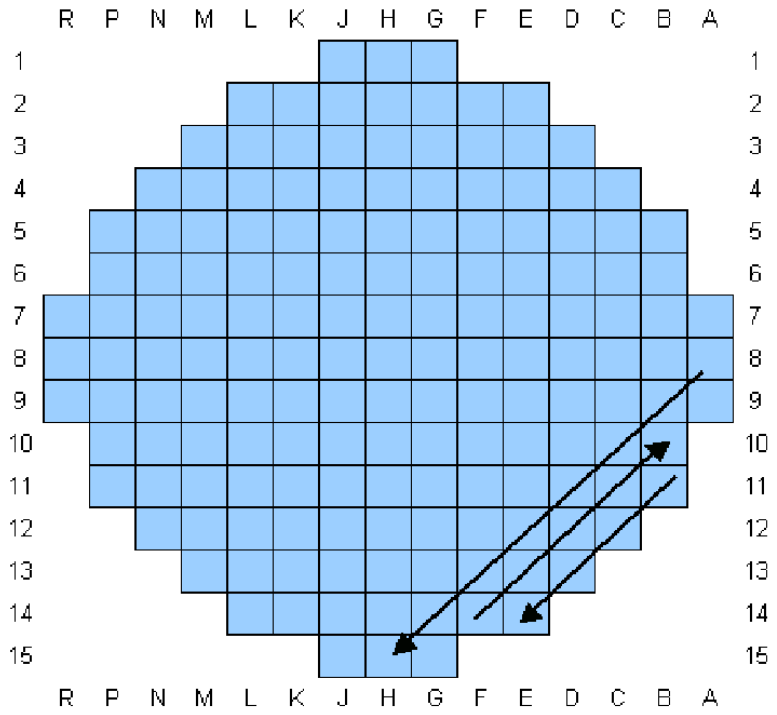

Figure 1.1: Serpent type loading pattern in a reactor analogous to the one in Dampierre-en-Burly [18]

though it did not have any real consequences on people or materials, it raised concern about the safety measures applied to core loading, in particular to monitoring. As a general rule for Pressurized Water Reactors (PWR) in France, loading processes are supervised via two proportional counters placed outside of the core, one on each side. Nevertheless, the readings taken from these detectors were deemed not enough for error prevention, as it was observed that the measured count rates did not correlate with the margin to criticality of the system, characterized by k_{eff} in Figure 1.2.

On the other hand, experiments performed in the GUINEVERE facility from 2012 onward, devoted to Accelerator Driven Subcritical Reactors, showed that the aforementioned correlation can be quite strong when the reactor is fed with a neutron source whose intensity changes over time [13, 5, 11]. The GUINEVERE facility, situated in the SCK·CEN research center in Mol, Belgium, coupled the fast neutron subcritical reactor VENUS-F to a time-dependent external neutron source consisting on the deuteron accelerator GENEPI-3C and a tritium target to ensure the conversion of deuterons to neutrons via the $T(d,n)\alpha$ fusion reaction. However, the experiments that took place there were performed for mostly symmetrical configurations of the VENUS-F core, quite different from those encountered during loading (see Figure 1.1). It was this fact that motivated the birth of the SALMON project (Subcritical Approach for core Loading MONitoring), with the objective of improving the monitoring of core loading by means of measuring the reactivity at several steps of fuel loading.

The first phase of this project consisted on the usage of the GENEPI-3C accelerator as

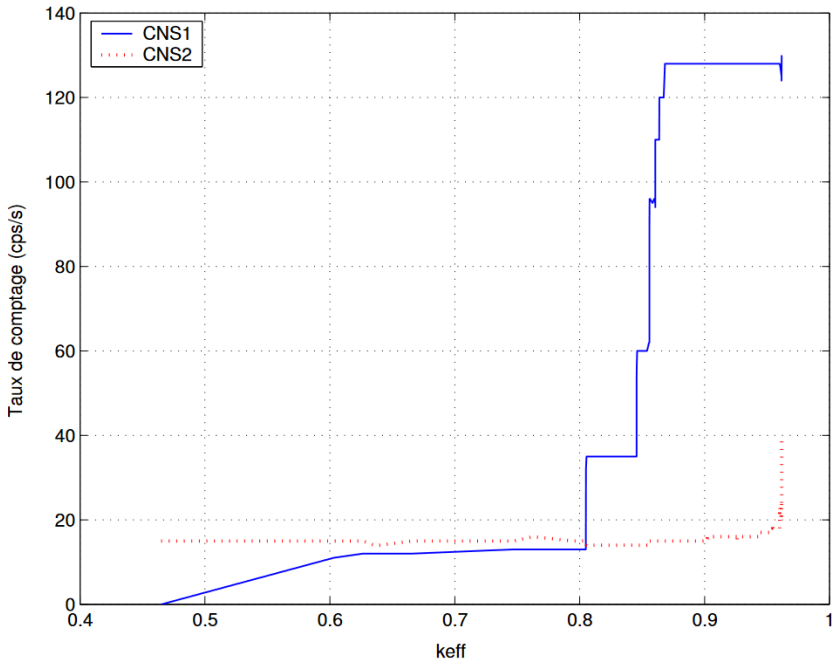

Figure 1.2: Evolution of count rates as a fuction of k_{eff} for both Dampierre detectors. k_{eff} obtained from simulations [18]

.

a Pulsed Neutron Source (PNS), coupled with the VENUS-F fast neutron reactor, whose core was configured to represent different steps of the loading process for which reactivity was estimated from the responses of ^{235}U fission chambers to neutron pulse injections in the reactor core. The result of this experiment was very promising, showing that despite spatial effects caused by both subcriticality and the asymmetry of the partially loaded core, the correlation between the measured reactivity and the one taken as a reference was remarkably strong. In addition to that, the used method was seen to be sensitive to loading errors, showing a lot of promise regarding their detection in a practical case [1].

In light of these favorable results, the second phase of the SALMON project follows, with the present work being part of it. This stage goes a step further, aiming to design a setting that is more representative of an actual PWR and to test the same methods used in the first phase on these new reactor configurations. In this context, this work consisted in evaluating the necessary changes that VENUS-F will have to undergo to become a thermal reactor (analogous to industrial PWRs), with a more realistic core configuration and loading plan. In addition to that, optimal detector positions and characteristics were also to be found, and finally, the validity of our measurement methods was to be assessed with the use of computational simulations of PNS experiment, via the *Serpent 2* neutron transport code.

Chapter 2

Fundamentals on Nuclear Reactor Physics and methodology

In this chapter, we fix the attention on the chain reactions that induce the controlled fission of the reactor fuel, and as a consequence, we also delve into the behavior of neutrons and the different ways they interact with atomic nuclei. The discussion is based predominantly on the Introduction to Nuclear Reactor Theory book, from J. R. Lamarsh [9].

At the end of the chapter, the objectives of this work will be further detailed, and a description of the methodology, tools and procedures used to attain said objectives will also be given.

2.1 Interaction of neutrons with matter

Being electrically neutral particles, neutrons mainly interact with the atomic nucleus, and the way they do it is greatly dependent on their energy [16].

The first main type of neutron-nucleus interaction is **scattering**, in which neutrons experiment a change in their speed and direction, and thus in their energy. Among this type of interactions, one can distinguish **elastic scattering**, where the total kinetic energy of the system remains constant and is only transferred, usually from the neutron to the nuclei, and **inelastic scattering**, where part of the total kinetic energy transforms into excitation energy of the scattered nucleus.

On the other hand, the mechanism that defines the second fundamental type of interactions is **compound nucleus formation**, which is the result of the absorption of the incident neutron by the target nucleus. If the latter is ${}^{A}_{Z}X$, the resulting compound nucleus will be ${}^{A+1}_{Z}Y^{*}$, with an excitation energy approximately equal to the sum of the incident neutron's kinetic energy and binding energy to the compound nucleus. In this state, the compound nucleus is unstable, and there are several de-excitation paths that it can follow.

This de-excitation usually happens with the emission of a particle, most commonly a γ-ray ((n, γ) reaction, also known as **radiative capture**), but sometimes also a neutron

(scattering) or even a charged particle ((n, p), (n, α) reactions).

Radiative capture is quite prevalent, making it the main competitor to the process that holds the biggest interest to us, **nuclear fission**, specially in heavy, fissionable nuclei.

Being the origin of the energy produced in nuclear reactors, fission happens mainly for very heavy nuclei (for example, Uranium) that break into two lighter nuclei, called fission fragments. This also results in the emission of a certain quantity of neutrons, as well as γ-rays, and a big amount of energy in the form of kinetic energy of the fission fragments, that later becomes heat when they slow down. This heat is what is used for the production of energy in nuclear power plants.

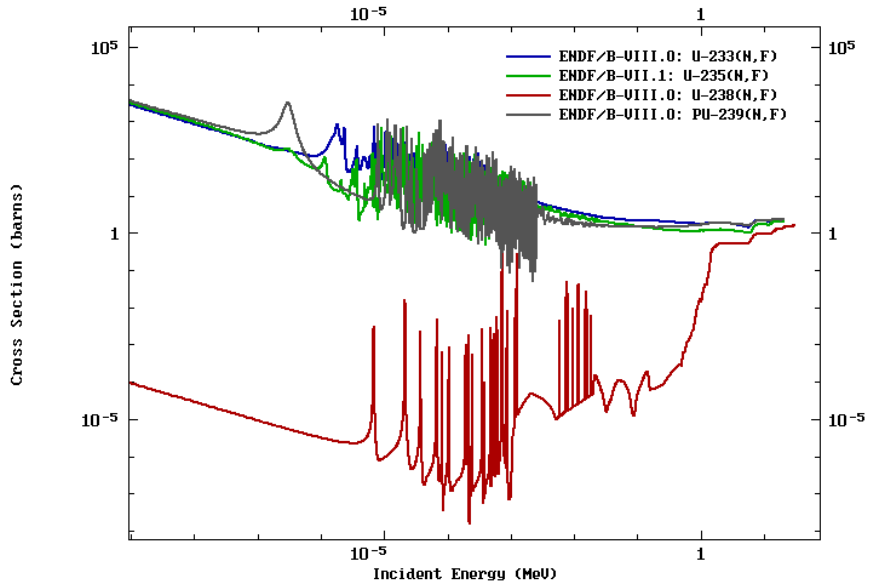

Figure 2.1: Evolution of the fission cross-section with energy for ^{233}U, ^{235}U, ^{238}U and ^{239}Pu, the main isotopes used as fuel in nuclear reactors. Figure obtained from the ENDF database [4, 3]

As it can be observed in figure 2.1, it is notable that in most cases the cross-section for fission is at one of its highest points when the neutrons have thermal energies (~ 0.025 eV), specially compared with other processes. This is what motivates the usage of this neutron energy spectrum in almost every power nuclear reactor, and this is achieved thanks to a moderator material, made of light nuclei like water or graphite, that slows down neutrons via elastic scattering.

In addition to that, two types of fissionable nuclei can be distinguished: the first one, usually called fissile nuclei, can undergo fission at any energy, which is the case for ^{235}U or ^{239}Pu. Other nuclei, like ^{238}U, have a certain energy threshold than incident neutrons must have to induce them to fission.

Despite de-excitation by charged particle emission being rare, there is one notable example in this context: the **reaction** $n +^{10} B \rightarrow \alpha +^{7} Li$, that has such a large cross-section that ^{10}B is used as a **neutron poison** to regulate chain reactions inside nuclear reactors.

2.2 Neutron chain reactions

As it was just discussed, fission reactions result in the emission of the so-called **prompt neutrons**, that can themselves interact with other fissionable nuclei inside a reactor and cause new fissions that release a new generation of neutrons and so on and so forth, resulting in a chain reaction. This is precisely what enables fission reactors to work, and quantifying it is of great importance for energy production purposes, especially for safety reasons. Therefore, the **effective multiplication factor**, k_{eff}, is defined as:

$$k_{\text{eff}} = \frac{\text{number of neutrons in a certain generation}}{\text{number of neutrons in the immediately preceding generation}} \tag{2.1}$$

For practical reasons, the **reactivity**, ρ, is derived from k_{eff} as:

$$\rho = \frac{k_{\text{eff}} - 1}{k_{\text{eff}}} \tag{2.2}$$

Due to its magnitude usually being very small, it is generally expressed in pcm, from the french "*pour cent mille*", that is to say, $\times 10^{-5}$.

Using these quantities, the operation modes of a reactor can be classified as follows:

- When $k_{\text{eff}} = 1$ and therefore $\rho = 0$, the reactor is said to be **critical**. This means that exactly one neutron per fission ends up triggering another fission event, which results in a stable, self-sustained chain reaction. This is the most desirable regime for classic nuclear power reactors, as it maintains a both steady neutron population and power output.

- When $k_{\text{eff}} > 1$ and therefore $\rho > 0$, the reactor is said to be **supercritical**. In this case, the neutron population, and consequently the power output increases at each new generation.

- When $k_{\text{eff}} < 1$ and therefore $\rho < 0$, the reactor is said to be **subcritical**. In this instance, the neutron population and power output will keep on decreasing at each new generation, until the chain reaction eventually dies out.

Another important parameter that is quite frequently used when talking about chain reactions is the **mean generation time**, Λ_{eff}, which is defined as the mean time between the emission of a neutron after a fission and its capture by another nucleus to trigger a subsequent fission. Its value is typically on the order of magnitude of $10^{-4} - 10^{-6}$ s, being much smaller for fast neutron reactors than for thermal ones.

Taking all of this into account, when aiming to have a neutron chain reaction under control, it is fundamental to establish a balance between the rate of neutron production and the rate of neutron disappearance from the system. The two main ways a reactor can lose neutrons are them **leaking** through its vessel, or them being **absorbed** by other nuclei than the fissionable ones, and these two processes are mainly dependent on the size

and composition of the reactor. At the same time, there are several ways for neutrons to be produced inside a reactor.

In addition to **prompt neutrons** created by fission and the ones coming from an external source, some fission fragments may undergo a β-decay to an unbound level of the daughter nucleus, which then decays again by neutron emission. The corresponding neutrons generally appear a long time after the prompt decay, which explains their denomination of **delayed neutrons**. The whole phenomenon can be quantified by the effective **delayed neutron fraction**, β_{eff}, defined as the ratio between the mean number of delayed and total neutrons emitted per fission. From here a new parameter is defined for convenience of usage, the **reactivity in dollars**, being $\rho_{\$} = \frac{\rho}{\beta_{\text{eff}}}$. Taking delayed neutrons into account is fundamental for control and monitoring of chain reactions, as it allows one to distinguish two different cases in a supercritical reactor:

- When $\rho > \beta_{\text{eff}}$ and therefore $\rho_{\$} > 1$, the reactor is said to be **prompt supercritical**. In this state, the increase of neutron population and power is too fast to be humanely controllable, becoming dangerous.
- On the other hand, when $0 < \rho < \beta_{\text{eff}}$ and therefore $0 < \rho_{\$} < 1$, the reactor is actually **prompt subcritical** and the supercriticality happens only due to delayed neutrons. This makes the neutron population rise slowly, so this state can be used to increase the power output of a nuclear reactor in a controlled way.

In practice, delayed neutrons are usually grouped between the ones whose precursors had similar decay constants, and every group j is associated with a delayed neutron fraction $\beta_{j\text{eff}}$, a group decay constant λ_j and a concentration of their precursors c_j.

2.3 Neutron transport inside a nuclear reactor

Knowing in detail the behavior of the neutron population inside a reactor is the basis for every subsequent calculations and measurements. In order to do so, one can start by characterizing a neutron by its position in space $\mathbf{r}$, its energy E and the direction of its movement $\mathbf{\Omega}$ at a time t, hence establishing the **neutron density**, $n(\mathbf{r}, E, \mathbf{\Omega}, t)$. Multiplying it by the velocity module, the **neutron flux** can be defined:

$$\Phi(\mathbf{r}, E, \mathbf{\Omega}, t) = n(\mathbf{r}, E, \mathbf{\Omega}, t)v \tag{2.3}$$

The time evolution of this quantity is described by the time dependent **Boltzmann Equation**, for which a thorough derivation can be found in previous works on the matter [1]. However, in its more general form this equation is too complicated to solve in a system as complex as a nuclear reactor, and even if done numerically the computational time is quite high. To address this issue, the neutron flux can be factorized in an amplitude factor $n(t)$ that holds the most part of the time dependence, and a form factor ψ with dependence on every variable, as follows:

$$\Phi(\mathbf{r}, E, \mathbf{\Omega}, t) = n(t)\psi(\mathbf{r}, E, \mathbf{\Omega}, t) \tag{2.4}$$

Furthermore, with the hypothesis of being close to criticality, an approximation can be made by considering the time dependence of the form factor negligible. This consideration allows one to obtain the **Point Kinetics Equations**, much more reasonable to handle and even analytically solvable in some conditions:

$$\begin{cases} \dfrac{d}{dt}n(t) = \dfrac{\rho - \beta_{\text{eff}}}{\Lambda_{\text{eff}}}n(t) + \displaystyle\sum_{j}^{J} \lambda_j c_j(t) + s(t) \\ \dfrac{d}{dt}c_j(t) = -\lambda_j c_j(t) + \dfrac{\beta_{j\text{eff}}}{\Lambda_{\text{eff}}}n(t) \end{cases} \tag{2.5}$$

where the quantities with the sub-index j correspond to the ones related to each of the delayed neutron groups, and *s(t)* refers to the intensity of an external neutron source.

It is important to note that even when the condition of being close to criticality is fulfilled, these equations are blind to flux deformations in position and energy.

2.4 Beyond Point Kinetics

When our interest falls out of the reach of point kinetics, like for example when studying spatial effects, a more realistic model can be achieved by implementing a modal approach, that is to say, by expressing the neutron flux as a sum of harmonics (often called α-modes), Φ_{α_i}. This results in the following expression:

$$\Phi(\mathbf{r}, E, \mathbf{\Omega}, t) = \sum_{i} T_i(t)\phi_{\alpha_i}(\mathbf{r}, E, \mathbf{\Omega}) \tag{2.6}$$

which is obtained from the resolution of the Boltzmann equation as an eigenvalue problem in α when assuming that the time dependence of the neutron flux can be separated in the following way: $\phi(\mathbf{r}, E, \mathbf{\Omega}, t) = \phi(\mathbf{r}, E, \mathbf{\Omega})e^{\alpha t}$ [2].

The case of taking only the first term of the sum, keeping only the fundamental mode α_0, corresponds to the case of point kinetics, and the fundamental eigenvalue is related to the reactivity in the following way:

$$\alpha_0 = \frac{\rho - \beta_{\text{eff}}}{\Lambda_{\text{eff}}} \tag{2.7}$$

It can be proved that in simple geometries, a point can be found where all the harmonics except the fundamental cancel out, meaning that finding that point in a certain system can be really useful for, among other things, placing a detector there and improving the accuracy of reactivity measurements [10]. However, in the case of wanting to tackle more sophisticated problems using this model, a really large amount of terms might be needed to properly describe all the physical effects involved. This is why this approach was historically not very explored, due to lack of computational power.

2.5 Pulsed Neutron Source (PNS) experiments

As it was discussed in the introduction, it has been observed that strong correlation between the evolution of count rates in a reactor and its reactivity can be found when it is fed by a time dependent neutron source. This the reason why a large amount of reactivity measurement experiments have been performed in subcritical cores coupled with an external neutron source whose intensity varies periodically. That is the case for the SALMON project, where the VENUS reactor receives neutrons from the GENEPI-3C accelerator. For the sake of representativeness, the time dependence of this neutron source has been chosen to be a series of periodic neutron pulses, as this is the most probable time structure to be used in an actual power reactor, due to the existence of commercial pulsed neutron generators. This is the origin of the denomination of **PNS experiments**.

A perfect pulsed source with a period T and n_P pulses in total can be described by the expression:

$$s(t) = \sum_{j=0}^{n_P-1} \delta(t - jT) \tag{2.8}$$

Even with a source like this, several hypotheses must be fulfilled to achieve a straightforward resolution of the system (2.5):

- On top of meeting the criteria for point kinetics, only one global delayed neutron group should be taken into account
- The frequency of the pulsed source f must be much larger than the delayed neutron group decay constant λ
- The total number of pulses n_p must be large enough to guarantee that the delayed neutron precursors arrive to equilibrium

In this conditions, the use of the Laplace transform to solve the Point Kinetics equations [5] leads to the following expression for the evolution of the neutron population:

$$n(t) \propto \exp\left(\frac{\rho - \beta_{\text{eff}}}{\Lambda_{\text{eff}}} t\right) + \frac{\Lambda_{\text{eff}}\beta_{\text{eff}}}{(\rho - \beta_{\text{eff}})\rho T} \exp\left(\frac{\lambda\rho}{\beta_{\text{eff}} - \rho}(t - T)\right) \tag{2.9}$$

2.6 The Area method (aka Sjöstrand method)

Examining equation (2.9), one can observe that the first term describes the very fast decay of the prompt multiplications after the pulse, while the second term refers to the decay of the multiplications triggered by delayed neutrons. This second decay is so slow that the neutron population can be considered basically constant on the milliseconds' scale. This behavior is represented in Figure 2.2.

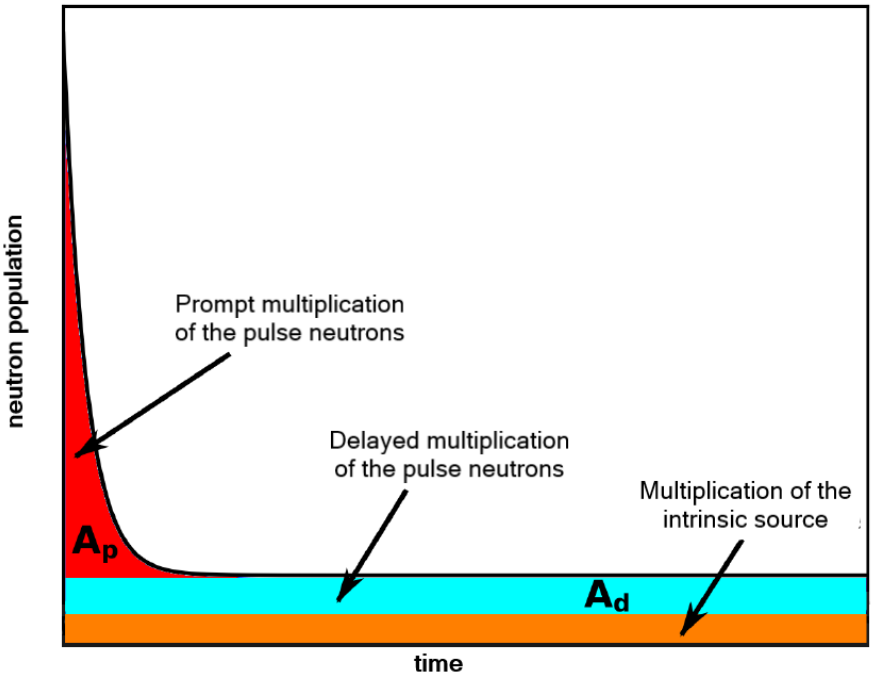

Figure 2.2: Representation of the time evolution of the neutron population in a subcritical system after a Dirac neutron pulse [1]

Via integration of expression (2.9) over time, one can find the following relations for the "prompt area" A_p and the "delayed area" A_d:

$$A_p = \frac{\Lambda_{\text{eff}}}{\beta_{\text{eff}} - \rho} \text{ and } A_d = \frac{\beta_{\text{eff}}\Lambda_{\text{eff}}}{\rho(\rho - \beta_{\text{eff}})} \tag{2.10}$$

Given this, as its name suggests, the Area method consists on the measurement of this two areas or, alternatively, A_d and $A_{tot} = A_p + A_d$, in order to calculate the reactivity in the following way:

$$\frac{\rho}{\beta_{\text{eff}}} = \rho_{\$} = -\frac{A_p}{A_d} = 1 - \frac{A_{\text{tot}}}{A_d} \tag{2.11}$$

The figure also shows a third possible area, which corresponds to an **intrinsic neutron** source. Indeed, in addition to fission, neutrons can appear in the reactor following radioactive decay of some nuclei, directly through spontaneous fission, or indirectly after α-decay followed by (α, n) reactions on other nuclei, such as ^{18}O and ^{19}F [15]. In the case of an intrinsic source being present, the measurement of the corresponding "intrinsic area" A_{int} will also be necessary in order to subtract it accordingly.

The reliability of this reactivity measurement method has been tested successfully in several experiments [13, 5, 11, 1], among which is the first phase of project SALMON, which is why it will also be the main option when tackling this second phase.

In spite of that, the need of using the delayed neutron level to calculate A_d generates two

important constraints. First the pulse frequency has to be chosen carefully for the pulses to be long enough to have a well established delayed neutron plateau, distinguishable from the prompt decay. Secondly, there has to be enough statistics for the delayed neutron level so the statistical fluctuations do not disrupt the calculation of its area. These constraints led to the proposition of an alternative method that focuses on the prompt decay, avoiding the need of the delayed neutron level.

2.7 The Derivative method

As it has been explained, the first term of equation 2.9 follows the decay of the prompt multiplications from the source neutrons. This means that if the delayed neutron contribution is subtracted from that expression, the logarithmic derivative of just the prompt term can be performed, giving:

$$\frac{1}{n_p(t)}\frac{dn_p(t)}{dt} = \frac{d}{dt}\ln n_p(t) = \frac{\rho - \beta_{\text{eff}}}{\Lambda_{\text{eff}}} \tag{2.12}$$

Then, given that β_{eff} and Λ_{eff} can be obtained via simulations with neutron transport codes or even measured, the reactivity might also be inferred from the prompt decay of the curve.

Nevertheless, in practice this is not as direct, as the point kinetics model proves to be too simplistic to apply in some cases. Indeed, it has been observed that when using the aforementioned modal approach in a simplified geometry, $\frac{dn_p(t)}{dt}$ is no longer constant, but the minimum of the log derivative remains equal to $\frac{\rho-\beta_{\text{eff}}}{\Lambda_{\text{eff}}}$, which could allow for an alternative reactivity measuring technique [10]. As opposed to the Area method, this one has not been used before in a context similar enough to ours to prove its effectiveness, so it presents an opportunity to test it.

2.8 Methodology

The purpose of the present work has been to design a new core for the VENUS-F reactor, more representative of PWRs, and to study the optimal instrumentation that should be used within it to perform reactivity measurements from PNS experiments. This has been done in preparation for future experiments that will be performed in this reactor, in order to assess their feasibility, analyze the constraints they will be subject to and test the effectiveness of the methods that will be used to measure reactivity. This section will go through the tools and the procedures that have been employed to attain this objective.

2.8.1 Software resources for simulation and analysis

The Monte Carlo simulations that form the bulk of this study have been performed using the neutron transport simulation code Serpent 2 [12]. This code is a versatile calculation

tool for reactor physics, as it allows to design the geometry and materials of a reactor and then perform a wide array of different simulations in said geometry, with the ability to tune every detail of them according to the particular needs of the simulation.

As a complement to Serpent 2, a suite of parsers named SerpentTools [8] allows for interaction with the different Serpent output files in a Python3 environment, for an ensuing manipulation and analysis of them using the different utilities and tools this language provides.

2.8.2 Simulation conditions and procedures

The simulations performed in this study can be clearly classified in two types. The first ones, referred as steady state simulations, do not require any time structure, and are used to calculate kinetic parameters like k_{eff}, β_{eff}, or Λ_{eff}. On the other hand, time dependent simulations are needed for studying pulsed experiments. This ones require the definition of a certain time structure in order to describe the behavior of the system over time, as well as a neutron source, and a number of detectors that can be designed to match any particular needs.

The characteristics of the simulated source were defined to be those obtained from the real GENEPI-3C accelerator: a quasi-isotropic source of 14 MeV neutrons with a pulse width of 1 μs.

However, it is important to note that Serpent does not allow for periodic source driven simulations, which is the aim. Keeping this in mind, the simulations were first carried out with a source of neutrons emitted at t=0.

The detectors for this simulations have been defined as fission chambers using ^{235}U or ^{238}U as a deposit. In order to reduce the variance of the simulation result, the time dependent count rates are calculated using the following expression:

$$R_f(t) = \iiint_{V_{det}} \int_{E} N_{depos}\sigma_f(E)\phi(\mathbf{r}, E, \mathbf{\Omega}, t)dEdV \tag{2.13}$$

where N_{depos} and $\sigma_f(E)$ are the nuclide density and the energy dependent fission cross-section of the detector deposit, respectively, ϕ is the time dependent neutron flux and V_{det} is the a cylindrical volume at the detector position.

The time response of the reactor was reproduced using a particular binning with 1 μs bins for the first 100 μs, then changing to a logarithmic binning until reaching 30 minutes. The hybrid binning was chosen to be this way with the aim of having high granularity in the beginning, where the prompt decay occurs, and then having a smaller amount of bigger bins for the rest, allowing faster calculations and reducing the chance of empty bins.

Finally, the detector time responses were subsequently convoluted with the periodic structure of the actual source. This periodic structure consists on multiple 1 μs wide neutron pulses with a certain frequency that has had to be adjusted to allow for the appearance of a clearly distinguishable delayed neutron level in the spectra.

Chapter 3

The case of a simplified cylindrical reactor core

3.1 Design of the simplified geometry

The first step on this work consisted in the design of a reactor core with a simplified geometry that would allow for familiarization with the software and techniques in place, but also specially for making tests with possible pulse frequencies and assessing the viability of the methods that would be used in the eventual real geometry in a way that would take less computational time and would be easier to navigate, while still providing with useful information.

Even when dealing with a simplified model, several design constraints had to be taken into account. The most important of them was that in our objective of building a thermal reactor, representative of a PWRs, the originally fast reactor VENUS-F needed the addition of a neutron moderator, but due to the way is it built, water could not be used as one. For that reason, the substitute moderator was chosen to be polyethylene, given that its most basic chemical structure, CH_2, is representative of water and acts in a similar way.

Another fundamental design constraint has to do with the reactor structure itself, as it is not viable to change some of the already existing parts. In particular, it is known that VENUS-F has an outer reflector and base made of lead that had to remain unchanged. In contrast, the reactor's upper reflector, previously also made of lead, could be replaced by one made of polyethylene, which can contribute to neutron moderation.

The cylindrical outer reflector made of lead was filled with a solid core made of a homogeneous mixture of the fuel, UO_2, and the moderator, CH_2. The proportions of the fuel mixture were first calculated to achieve criticality, e. g. k_{eff}=1, with this configuration via steady state simulations, obtaining that 93.578% of the volume had to consist on polyethylene leaving a 6.422% of UO_2. After this, a central, cylindrical void shaft was added, in representation of the place were the accelerator responsible for the pulsed source would be.

Here, our third restraint appears. The aim is to design an accelerator driven system,

for which we need a certain margin of subcriticality, which in this case was set to be 0.95, allowing us to explore the full range of a loading process. As the central hole did not reduce the k_{eff} enough to arrive at that reasonable subcriticality, a layer of pure polyethylene was added between the lead reflector and the fuel, reducing the fuel volume and thus the $k_{\text{eff}}$to a value of 0.9521 ± 0.0002 . The final configuration is represented in figure 3.1.

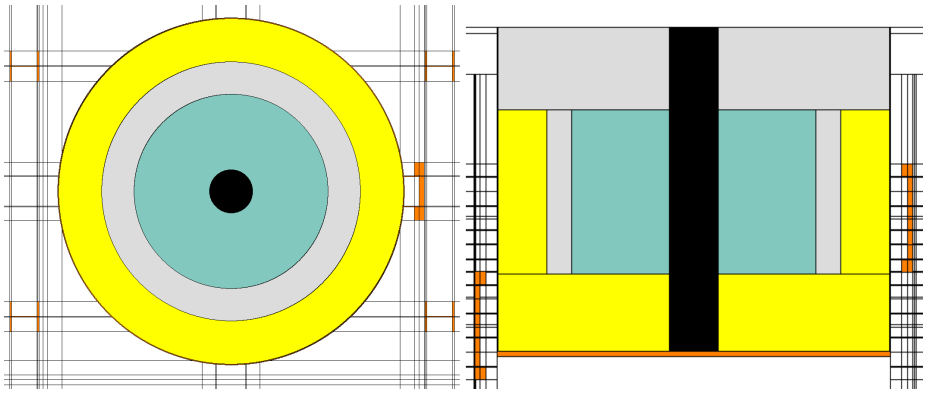

Figure 3.1: View from above (left) and from the front (right) of the simplified core geometry, with lead in yellow, polyethylene in gray and the fuel-CH_2 mixture in green.

As a reference, the radius of the depicted core is 80 cm, from which 20 cm are occupied by the lead reflector, 10 cm by the outer CH_2 layer, 40 cm by the fuel-CH_2 mixture and 10 cm by the shaft. The height of the core is also 80 cm, of which each reflector occupies 15 cm, while the mixture ocuppies the remaining 50 cm.

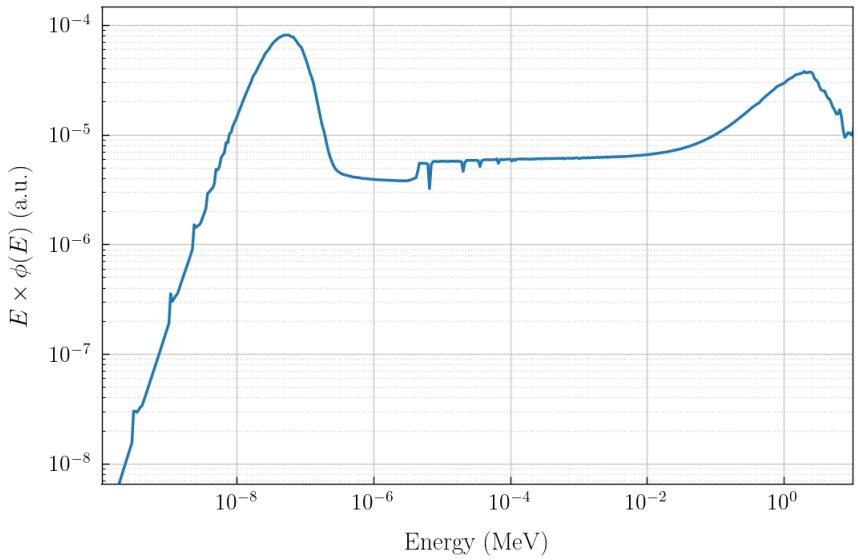

Figure 3.2: Energy distribution of the neutron flux in the simplified cylindrical core.

Figure 3.2 shows the neutron energy spectrum in the fuel-CH_2 mixture. As expected, two bumps can be observed, the one in the left corresponding to thermal neutrons ($\sim 10^{-7}$ MeV), while the one in the right is due to fission neutrons that just appeared in the core.

3.2 Reactivity measurements and testing

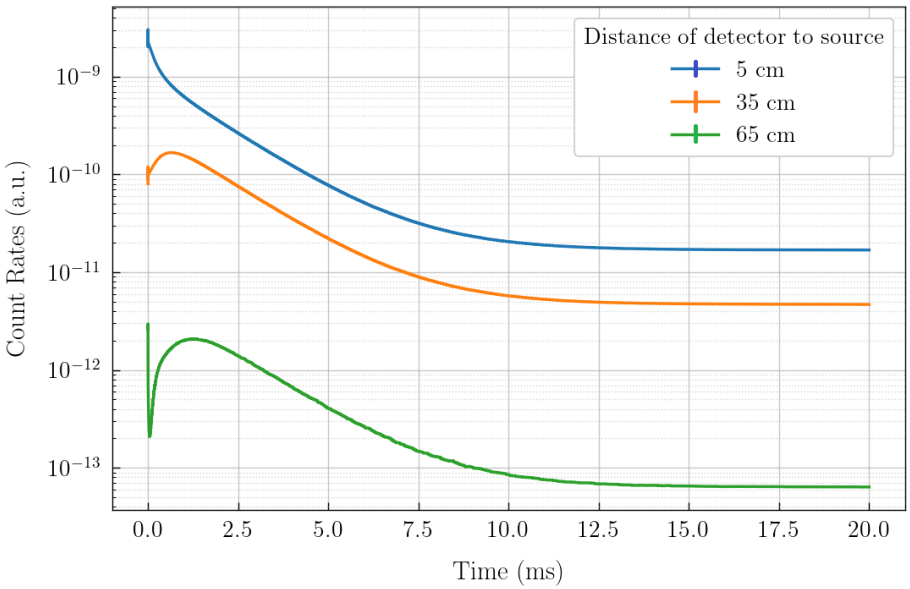

Figure 3.3: Time evolution of the count rates after one pulse in the simplified cylindrical core for cylindrical detector situated at three different distance and for a source of 20 Hz of frequency.

Time-dependent simulations were performed using an external source of 14 MeV neutrons, as described on the previous chapter. The detectors were defined as several concentric cylindrical sections, and the time evolution of the count rates was then folded with the periodic pulse structure, for which different frequencies were tried out, until one of 20 Hz was decided, as it allowed for a well distinguished delayed neutron level for every considered cylinder. The result of these simulations and foldings can be seen in Figure 3.3 for three of the concentric cylinders at different distances to the source, with the first one falling in the fuel part, the second in the polyethylene ring and the third in the lead reflector. These results serve an essential purpose, to check if the delayed neutron plateau is properly reached in order to be able to utilize the area method.

As these spectra are the result of a convolution, their error bars were calculated by resampling their pre-convolution values 1000 independent times, using a gaussian centered on the value itself and with an amplitude of its uncertainty given by the simulation. Then, the convolution was applied to each resampling, and the standard deviation of the 1000 results for each point was taken as its post-convolution uncertainty.

With the aim of identifying if the chosen time binning was affecting the convolution result, simulations were performed in the same conditions as before but doubling the amount of time bins assigned to the detectors. The result of this test can be seen in Figure 3.4.

It can be seen that doubling the amount of time bins used in the simulation does not improve or change in any other way the shape of the time histogram, nor the quantities calculated from it, so keeping the original binning was decided, as it reduced the time consumption of the simulations by a factor of 4.

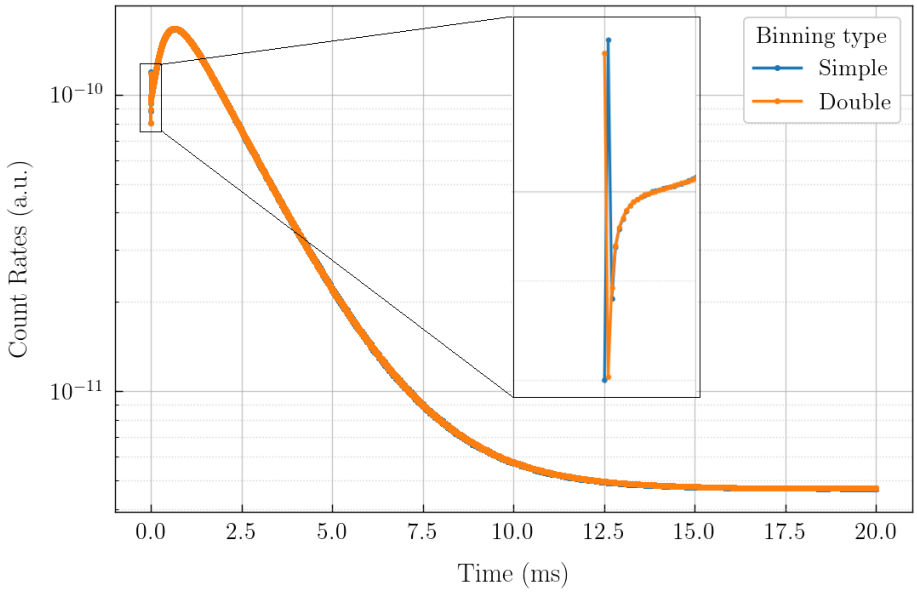

Figure 3.4: Comparison of time evolution of the count rates rates over one pulse in the simplified cylindrical core for a source of 20 Hz of frequency with two different time binnings, one having double the bins than the other.

Even though the count rates show the expected shape, similar to the one in Figure 2.2, an unanticipated peak appears at the very beginning of the pulse. In order to identify the reasons behind the appearance of this pulse, the previous double binning results were first analyzed. In Figure 3.4 it can be observed that the appearance of the unexpected peak doesn't depend on the binning, so a physical origin was hypothesized.

In addition to that, new simulations were carried out, not handling the fission reactions and substituting them by neutron absorption. The results of those simulations it can be seen in Figure 3.5.

As expected, the count rates drop sharply when fission is not handled. However, the initial peak can still be observed, which led to the proposition of it being caused by the 14 MeV neutron source being detected directly, before interacting in any other way. Indeed, when calculating the time taken by 14 MeV neutrons from the center of the cylinder to the cylindrical detector layers, the result was in agreement with the position of the initial peak observed in every case, confirming our hypothesis.

Following this tests, and with the objective of mimicking the loading of a core, several simulations were made reducing the thickness of the fuel part of the core and replacing it with polyethylene. Then the area method was applied to the results of these simulations, calculating $\rho_\$$ for each core thickness.

The results of those calculations are compared in Figure 3.6 with the values given by steady state calculations for each of the simulated fuel volumes[1].

The area method results are remarkably close to the steady state ones for the detector

[1] A zoom is made to the area of interest for clarity, as values outside of it varied greatly and made the more relevant ones hard to see.

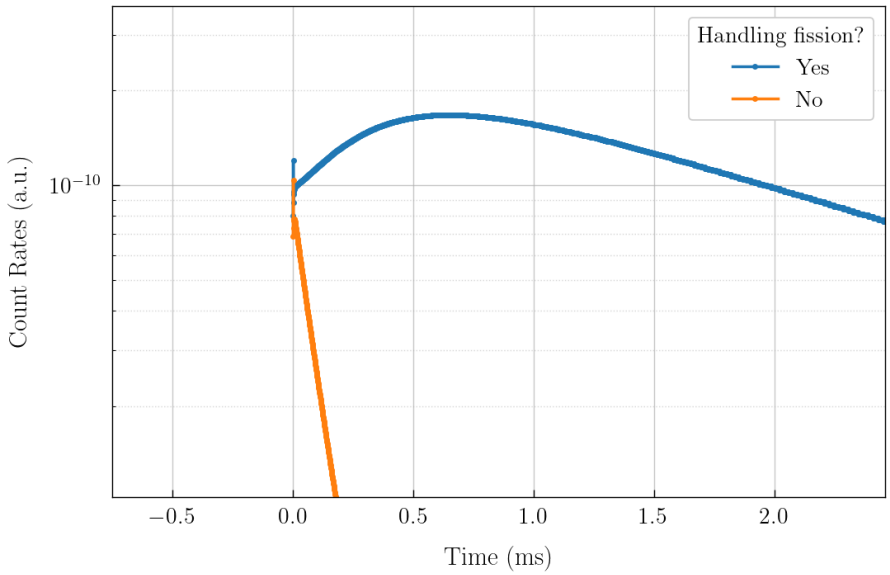

Figure 3.5: Comparison of time evolution of the count rates rates after one pulse in the simplified cylindrical core for a source of 20 Hz of frequency between a standard case and one when fission has not been taken into account.

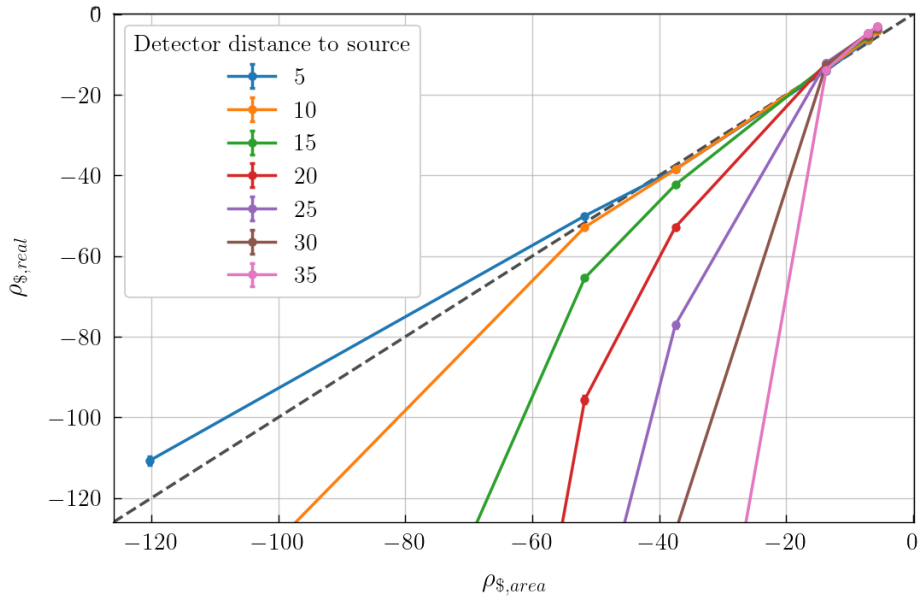

Figure 3.6: Comparison of the evolution of $\rho_\$$ as a function of the volume of fuel in the simplified cylindrical core between the steady state calculation and the area method result for detectors at different depths.

closer to the source. The results from the rest of the detectors are not as accurate, but still show a good correlation with steady state calculations, which is promising. Nevertheless, for configurations with low reactivity, low statistics for the delayed neutron level cause it to have a large statistical fluctuations, and thus increasing the error on the calculation of the area under the delayed neutron plateau. As a consequence, it is hard to draw a precise conclusion for those cases.

Chapter 4

Design and simulation of a realistic thermalized core for VENUS

4.1 Design of the core and loading plan

After having tested all the tools and methods in the simplified core geometry, what followed was the design of the real geometry for the thermalized core of VENUS-F. To begin with, the detailed descriptions of geometries and material corresponding to the room where VENUS-F is placed, up to the cylindrical lead reflector surrounding the core, were taken directly from the input files used in the first phase of the SALMON project, as all of them will remain unchanged for phase 2. On the other hand, the core itself was designed from scratch, with a basis on the specifications on composition and geometry of the fuel pins available and the GUINEVERE facility.

It is expected that, eventually, the experiments will be performed with a core containing a variety of different fuel types, ranging from UOX (Uranium based fuel) to MOX (Plutonium based fuel), but constrained to the specific fuel pins located in the facilities. As a starting point, it was decided that this work would study a pure UOX core, with an enrichment in ^{235}U of 3.3% in weight, as pins of these characteristics can be found among the available ones at SCK·CEN.

The fuel pins were grouped in square assemblies and surrounded by the moderator, polyethylene, with the purpose of loading full fuel assemblies at once, making the process more manageable. Different combinations of assembly sizes and quantities were studied, with the best fit finally being a structure of 12x12 fuel assemblies, themselves being composed of 6x6 fuel pins, all of them surrounded by pure polyethylene until all the space was filled. This structure was chosen taking into account the dimensions of both the reactor vessel and the fuel pins, finding a combination that would allow good symmetry and a number of fuel pins representative of the one in a PWR. In addition to that, a void hole with the size of four fuel assemblies was added in the middle to allow the insertion of the GENEPI-3C accelerator.

Regarding the detectors, cylindrical spaces were reserved for them in each corner of

the core, replacing one fuel assembly each. From now on, this detector will be referred as *tl* (top left), *tr* (top right), *bl* (bottom left) and *br* (bottom right). A much smaller space, inside the core itself and nearby one of its diagonals, was assigned to the named *mini* detector, that takes the place of a singular fuel pin. Finally, two more spaces on the reflector, that had already been used for detectors during phase one of SALMON were given to the *left* and *right* detectors. The detector locations can be seen in figure 4.1, where they are marked with stars, and an arrow in the case of the *mini* one.

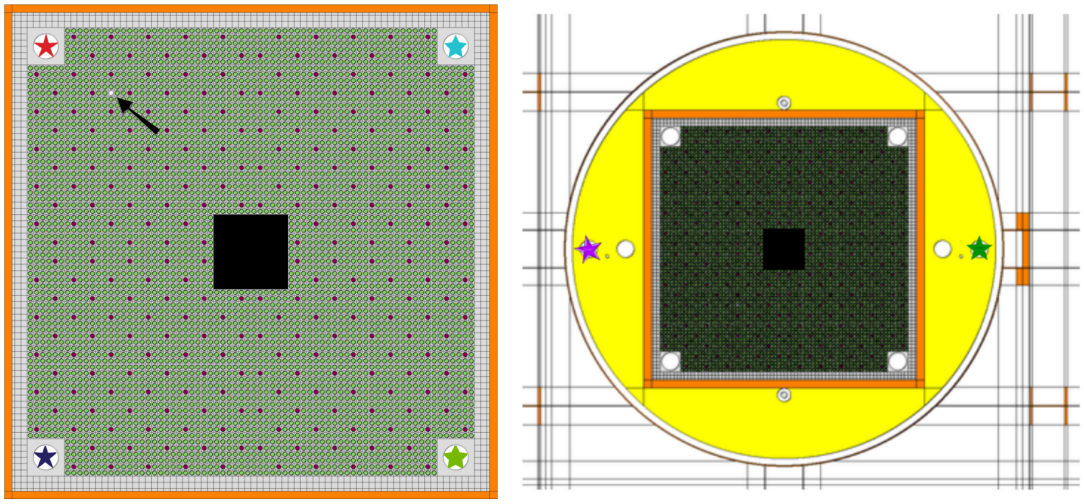

Figure 4.1: Final geometry of the designed thermalized core of VENUS-F seen from above, with the places occupied by detectors marked. Yellow corresponds to lead, orange to stainless steel, gray to polyethylene, green to UOX fuel, purple to B_4C.

As previously discussed, the seven detectors were designed to be fission chambers, and the option of them using either ^{235}U or ^{238}U as a deposit was implemented, as a way to test the response of each of them.

Steady state simulations were run to calculate the k_{eff} of the core in this state, and it was found to still be slightly supercritical. To address this issue, it was decided to introduce a "neutron poison" in the form of B_4C pins replacing some of the fuel ones in each assembly. After several tests, the optimal amount of them to arrive to a reasonable subcriticality of 0.9597 ± 0.0003 was found to be 2 per assembly, and they were arranged throughout the core in a way that kept its symmetry. The final core geometry can be seen in figure 4.1, and includes a total amount of 136 fuel assemblies (to be compared to a typical 157 FAs in 900 MWe PWRs), amounting to 4624 fuel pins and 272 B_4C pins.

From the fully designed core, partially unloaded core configurations were also prepared, substituting one assembly at a time by a solid block of polyethylene, row by row and following a zig-zag pattern that is often used in the loading of real PWRs. Steady state calculations were run for each of the geometries to get their kinetic parameters. Then a select few of those geometries, eight in total, were chosen to perform PNS simulations in them. In particular, the most reactive configuration was chosen to be the one with half of the total assemblies in, and from there first full assembly rows and then just half rows were

emptied, ending with just half of the last assembly row in. The choice of the starting point was made because simulations of configurations with more fuel assemblies took lengthy amounts of time without adding much relevant information. The fullest and most empty configurations are represented in figure 4.2. The procedure and parameters were the same that were used for the simplified model, including the pulse frequency of 20 Hz, that was found to be the most adequate.

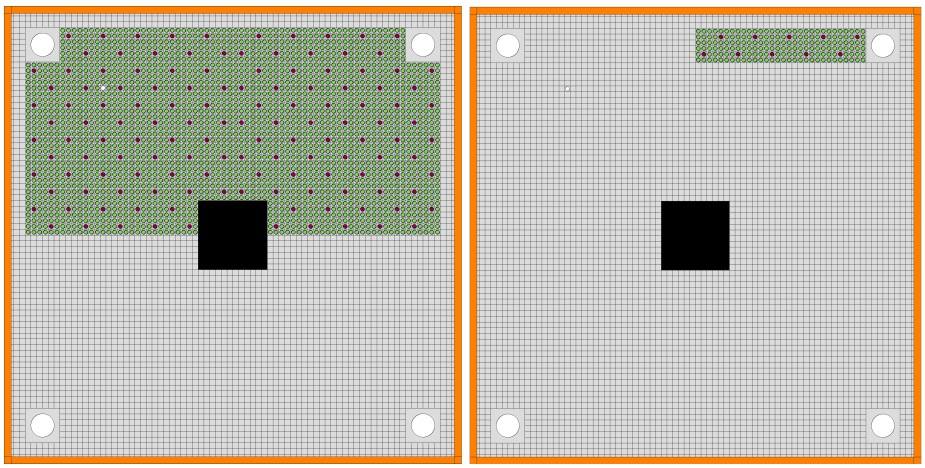

Figure 4.2: Geometries of the fullest and most empty configurations on the loading steps of the designed thermalized core of VENUS-F seen from above. Yellow corresponds to lead, orange to stainless steel, gray to polyethylene, green to UOX fuel, purple to B_4C.

With the purpose of getting an idea of the real count rates that would be obtained in a certain amount of experiment time, the obtained time histograms were properly normalized taking into account that the original spectra show values per source neutron, via the following expression:

$$CR_{real} = CR_{simul}\, I_{acc}\, m_{depos}\, t_{exp}\, f \tag{4.1}$$

where I_{acc} is the intensity of the GENEPI-3C accelerator, that is, the number of neutrons sent per unit of time, known to be of 10^6 neutrons/pulse; m_{depos} is the detector deposit mass; t_{exp} is the experiment time and f is the pulse frequency. An example can be observed in Figure 4.3, where the values were calculated for one hour of experiment and 1 mg of ^{235}U detector deposit.

This figure also illustrates the increase of statistical fluctuations on the delayed neutron level for configurations with lower reactivity, that has been linked with a worsening of the area method results. It is noteworthy that the sharp peak that can be seen in Figure 3.3 close to t=0 does not appear in this case, as the detectors are too far away from the source for any neutrons to arrive to them without interacting.

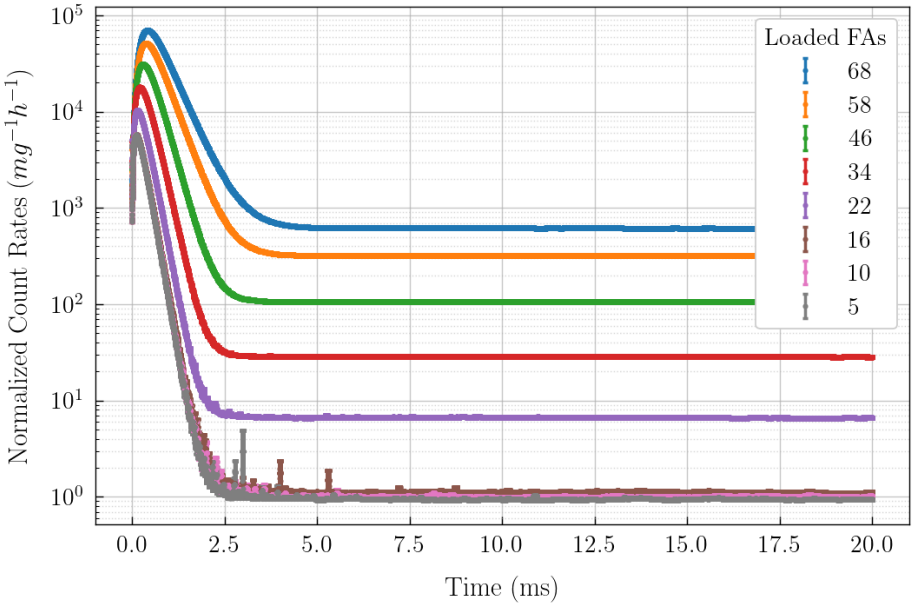

Figure 4.3: Time evolution of count rates after one pulse in the final geometry for the top left detector and different loading steps.

4.2 Simulation of reactivity measurements

Equivalently to what was done for the simplified geometry, the reactivity was calculated for each loading step and for each detector using both the area method and the derivative method.

The correlation between the $\rho_\$$ calculated via the area method and the one given by steady state calculations can be seen in Figure 4.4 for every different detector position and the two studied detector deposits: ^{235}U and ^{238}U[1].

The first thing that can be extracted from them is that not only a correlation clearly appears, but also some of the calculated values are in very good agreement with the real ones. This agreement is held much better when using ^{235}U as a deposit. Furthermore, the agreement is retained much longer by the detectors in direct contact with the fuel due to the order of the loading, namely *tl*, *tr* and *mini*. Moreover, the loss of correlation is much more notable for the detectors *bl* and *br* than for *left* and *right*,with as the latter staying closer to the fuel during the fullest loading steps. Indeed, during SALMON phase 1, it was seen that correlation between area method results and real ones was much better when closer to the fuel due to neutrons coming directly from the source of from scattering being mistakenly detected as prompt neutrons from fission. When far away from fuel, the ratio between prompt and source neutrons decreases, negatively affecting the results. This could also explain the better results obtained for a ^{235}U, as the fission threshold from ^{238}U decreases even further the contribution of lower energy neutrons from fission, favoring the

[1]Again, a zoom is made to the area of interest for clarity, as values outside of it varied greatly and made the more relevant ones hard to see.

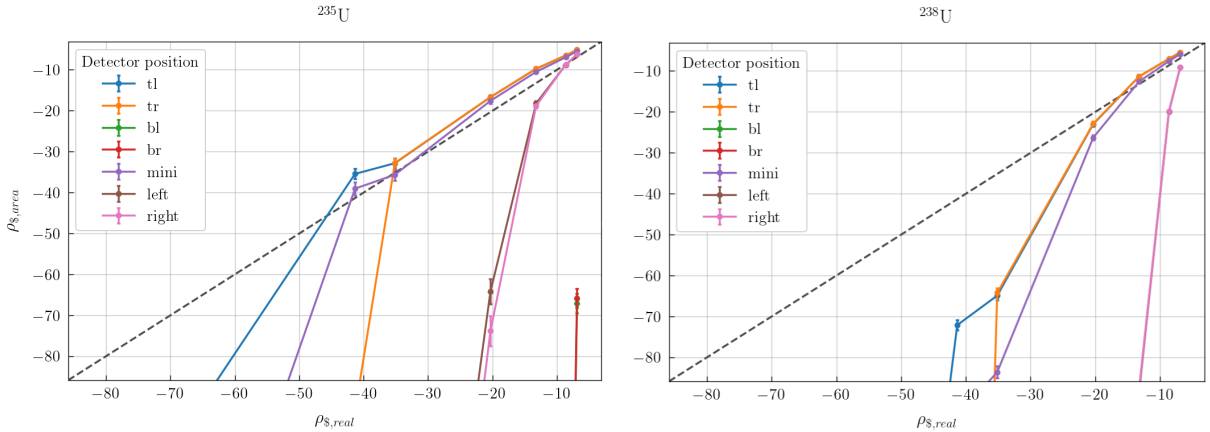

Figure 4.4: Comparison of the value of $\rho_\$$ from steady state calculation and from the area method result for each of the detector positions and for a ^{235}U deposit (left) or a ^{238}U one (right).

more energetic source neutrons.

Lastly, in the same way as in the simplified cylindrical model, the lack of statistics in low reactivity configurations makes the error bars become too big to draw any precise conclusions on either agreement to real values or even correlation.

For the derivative method, the count rate curves had to be first treated, subtracting the delayed neutron level from them and isolating the part where the prompt decay happens. In addition to that, numerical derivative methods are very sensitive to the statistical fluctuations that can be found in the curves due to them originating from a Monte Carlo simulation, so we applied a Savitzky-Golay filter to the data, a technique that allows to smooth them without distorting their tendency, and therefore improve the results [14].

Furthermore, real data collected during the first phase of the SALMON project was also treated and the novel derivative method was applied with the aim of finding out if effects present only in simulations were modifying the obtained result. Using all of this calculations, the effectiveness of both methods and their limitations where evaluated.

The following figures illustrate the different results obtained when studying the derivative method, with Figure 4.5 presenting the actual shape of the logarithmic derivatives of the prompt decay. The expected plateau appears, from which we can obtain the value of $\alpha_{min} = \frac{\rho - \beta_{\text{eff}}}{\Lambda_{\text{eff}}}$. At is was commented before, the lack of statistics for low reactivity configurations greatly affects the results obtained for them, in this case making the mentioned plateau much less distinguishable and thus the value of α_{min} much less accurate.

Figures 4.6 and 4.7 evaluate the derivative method using simulation results first, followed by real data collected on the phase 1 of the SALMON project. Looking at the simulation results, it can be noted that for high reactivities, there is a good correlation between derivative method values and reference ones, but this correlation is lost as reactivity decreases. Even though the real data, corresponds to a different experiment, his same loss of correlation can be seen in an even sharper way which reaffirms the low reliability that the derivative method seems to have. It is for this reason that its usage can be completely discarded.

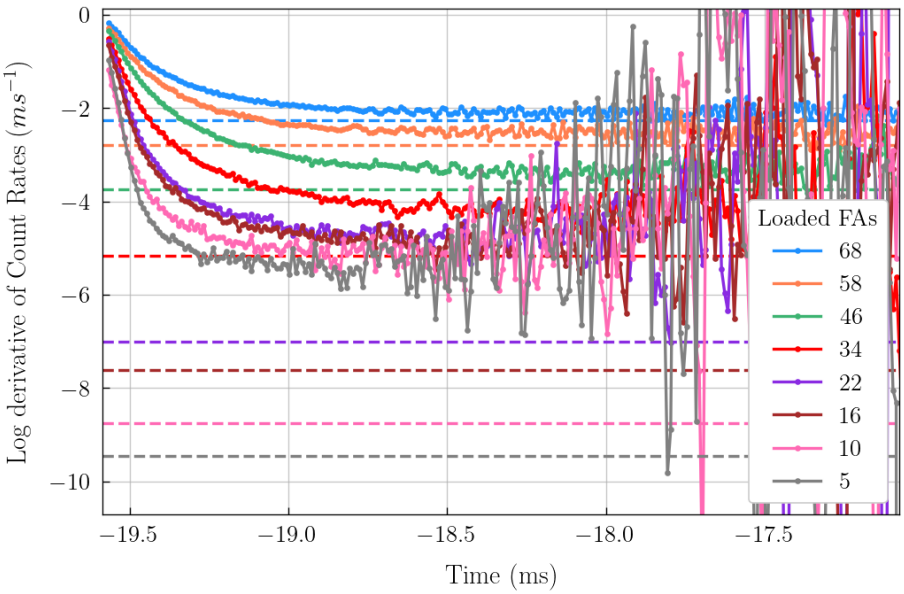

Figure 4.5: Numerical logarithmic derivative of the prompt decay for eight selected loading steps, compared with the value of α_{min} for each of them (in dotted line).

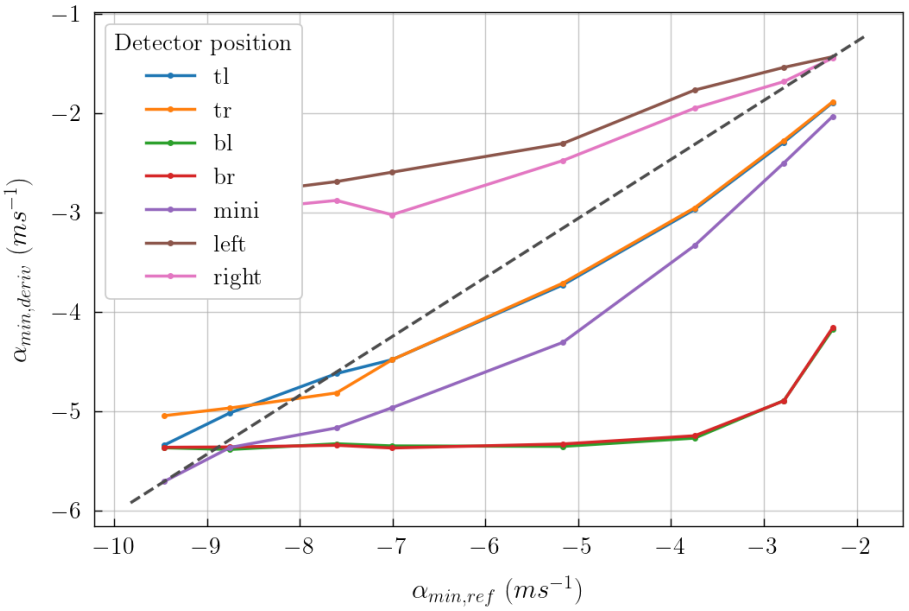

Figure 4.6: Comparison of the value of α_{min} from steady state calculation and from the derivative method result for each of the detector positions.

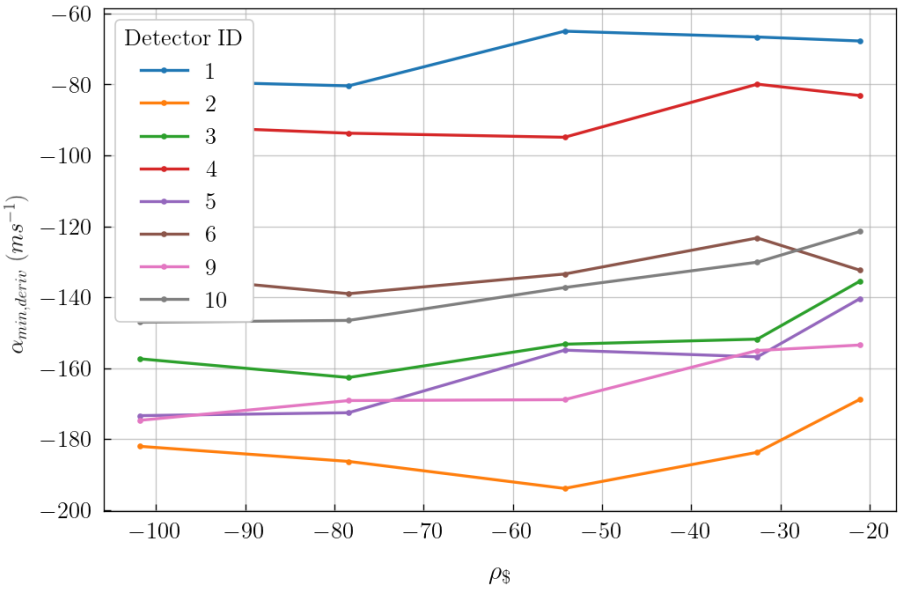

Figure 4.7: Comparison of the measured value of $\rho_\$$ and the value of α_{min} from the derivative method result applied to data collected on SALMON phase 1 for several detectors.

4.3 Assessment of constraints and optimizations

As discussed in section 1.4, it might be possible to find a point in the geometry were all the neutron flux harmonics cancel out except the fundamental. This would be ideal as a detector placed in that point would provide the exact measurement of the reactivity at least for one full configuration, opening the door for using it as a reference value. More simulations where run with the core fully loaded and varying the *mini* detector's position along on of the core's diagonals. Then, $\rho_\$$ was calculated using the area method, and that value was compared with the one obtained from the steady state calculation with the same configuration. The point where those two values where the closest would be the optimal point to place the *mini* detector inside the reactor core.

This pin position was found beside one of the diagonals of the core, at 13.35 cm from the source, where the values for $\rho_\$$ from steady state calculations and from the area method were almost equal. This point was then deemed the ideal one to place the *mini* detector in the eventual experiment.

Two well defined constraints had been identified regarding the eventual experiment: firstly, the fission chambers' instantaneous dead time would put a limit on the maximum number of counts per second that the detectors would reasonably be able to read. Looking at the detector response from previous similar experiments, it was deemed that 3×10^5 counts/s for the peak of the spectrum was an adequate upper limit to avoid serious dead time problems, that concentrate in that very peak, so this number was used in the calculation of the detector deposit masses displayed in Figure 4.8. This figure includes the exact optimal masses, as well as the most reasonable match from a limited list of available deposit masses that only include 1, 10, 100 and 1000 mg.

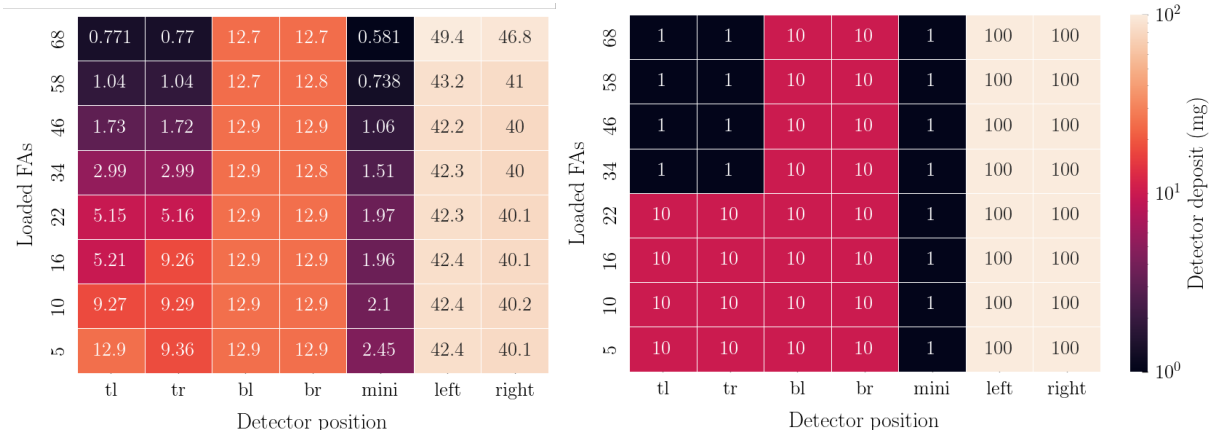

Figure 4.8: Heatmaps of the calculated optimal deposit masses (left) and the most adequate ones from the available selection (right) based on the detector dead time constraint for every detector position and selected configuration.

As expected, the detectors closer to the fuel call for smaller deposit masses. The exact calculated deposit was not the only thing taken into account when choosing from the available detectors to elaborate the figure in the right, but also their abundance, as detectors with lower deposit masses are more scarce. In the case of only being able to use a 1 mg deposit detector, it would be reserved from the *mini* one. It is noteworthy that even with this limitation in place, dead time will most probably still be an issue in the eventual experiment, so dead time corrections will have to be applied, usually with the *mini* detector as a reference, as its smaller volume makes it less sensitive to dead time.

The second constraint that was faced came from the necessity of having sufficient statistics in the measurements so as to reduce the uncertainty as much as possible for the delayed neutron level, in order to have it well defined. Nevertheless, that would condition the necessary experiment time, that should be kept within a reasonable level. In consequence, once the deposit mass was imposed by maintaining a reasonable dead time, the numbers of counts needed to arrive to the minimum experiment times necessary to attain a 0.5% statistical uncertainty for the delayed neutron level were calculated for every detector and loading step, followed by the experiment times necessary to attain said numbers of counts. This results are collected in Figure 4.9.

On one hand, it can be observed that for lower reactivities, some detectors would require a completely unreasonable amount of time to obtain enough statistics. For every loading step considered there is at least one detector that can get the necessary statistics in a decently low number of hours, opening the possibility of reducing the uncertainty even further if given enough time. In particular, the only detector that does this for the least reactive step is *tr*. This happens because the mentioned step includes only the right half of the last row of assemblies, making this detector the only one still in direct contact with the remaining fuel.

The fuel being used in this reactor model is UOX, from which the most part is ^{238}U. This isotope acts as an intrinsic neutron source due to spontaneous fission, and given its reaction rate and the abundance of it in this system, it is important to calculate its

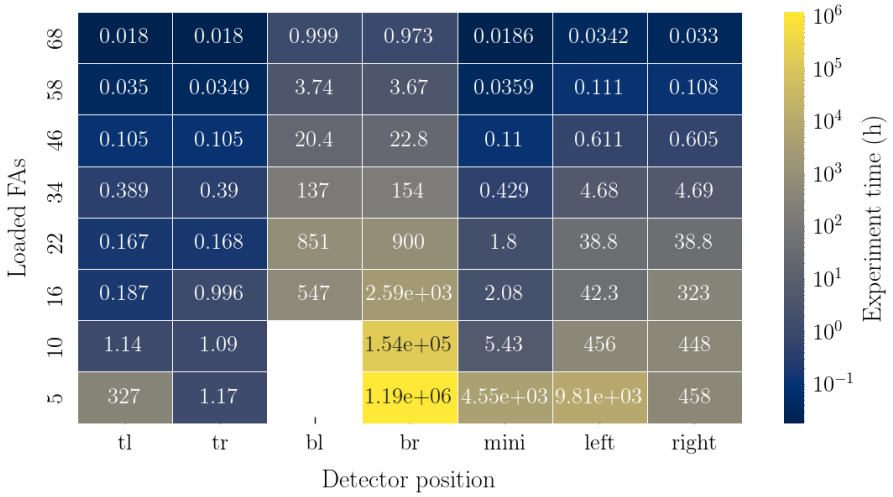

Figure 4.9: Heatmap of the calculated minimum experiment time based on the statistical uncertainty constraint for every detector position and selected configuration. Empty spaces correspond to very high times that are completely unachievable.

contribution as it may not be negligible in comparison with the delayed neutron level. [2] The intrinsic source contribution was calculated with simulations were the 14 MeV neutron source was replaced by neutrons coming from the spontaneous fission of ^{238}U.

Isotope	**Relative abundance (% in weight)**	**Spontaneous fission rate (neutrons/$(g * s)$)**
^{235}U	3.3	0.0003
^{238}U	96.6	0.0136

Table 4.1: Comparison of relative abundance in the fuel and spontaneous fission rate between ^{235}U and ^{238}U [17].

The count rates corresponding to the ^{238}U intrinsic source can be compared to the ones associated with delayed neutrons, with the ratio between the two being shown in Figure 4.10. From them it can be collected that due to the abundance of ^{238}U in the system, the intrinsic source absolutely cannot be neglected. Not only it represents a significant fraction of neutron counts in the delayed neutron plateau at high criticalities, but it also decreases at a lower rate than them as the criticality diminishes, so it becomes even higher for more subcritical configurations. This implies that in the eventual experiment, the intrinsic source will have to be measured while the reactor is off and taken into account in the reactivity measurements.

[2] Even though spontaneous fission also appears in ^{235}U, its lower reaction rate and relative abundance in the core allows us to neglect its involvement.

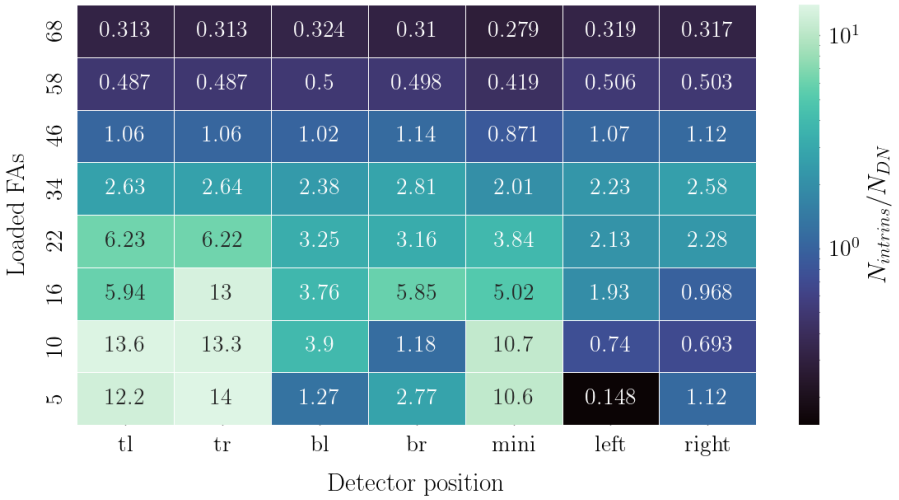

Figure 4.10: Heatmap of the ration between the count rates resulting from the U_{238} intrinsic source and the delayed neutrons for every detector position and selected configuration.

Chapter 5

Conclusions

This work consisted on the design of a new core for the VENUS-F reactor, adapting it to work with thermal neutrons and in general focusing on making it representative of a real Pressurized Water Reactor, like the ones used in nuclear power plants. This has been done with the objective of carrying out reactivity measurements during Pulsed Neutron Source experiments, so simulations of those experiments were performed, where the measuring methods and instrumentation were put to test. The detectors that would be used for that purpose have also been studied, establishing their positioning, type, deposit type and mass. Possible constraints originating from either the detectors or the reactor itself were evaluated, and in general the feasibility of the eventual experiment was appraised.

The first evaluated method has been the **Area Method**, which has already proven to work on previous experiments and it can be concluded that its is still effective for this one, as it maintains an overall good correlation and even good agreement between measured and reference values for the reactivity. Nevertheless, it can also be observed that this method is remarkably sensitive to having low statistics for the delayed neutron level, as it greatly increases the uncertainty on the calculation of that area, hindering our ability to draw conclusions about those cases. In order to draw more precise conclusions for deep subcritical configurations, simulations would have to be improved by using variance reduction methods or by letting them run for longer amounts of time.

What has been confirmed is the importance of choosing good detector positions, trying to keep as many of them as possible as close as possible to the fuel, specially in the loading steps where a low amount of assemblies are inside the core. In addition to that, it has been found that the ^{238}U intrinsic source has to be taken into account, measured when the accelerator is off and subtracted from the PNS spectra, to avoid its interference with the area method results.

As a possible alternative to the area method, the **Derivative Method** has also been studied. Unfortunately, even though it showed initial promise with satisfactory correlation between measured and reference values, this correlation has been seen to be lost for low values of the reactivity, most probably due to the amount of present harmonics being really high, specially for configurations with lower reactivities, and therefore one of the main requirements for the method to work not being met. Indeed, this method's effectiveness

decreases in the same situations as the area method, and this, joint to the fact that it requires a deeper, more complicated preparation of the data before being applied, led to it being completely discarded in favor of the more convenient and still quite functional area method.

Two clear constraints have been found that will affect the eventual experiment: firstly, the dead time of the detectors limits our choice on their deposit masses, choice that was already reduced to the available selection of said deposit masses. Due to the scarcity of detectors with a low deposit mass, it was concluded that they should be reserved for the detectors that have a bigger exposure to fuel, as they will always measure the highest count rates. It is also important to note that even in that case, a dead time correction will be necessary. A balance has to be found between having enough statistics on the delayed neutron level in order to maintain the effectiveness of the area method, and not having too many counts in a small amount of time to avoid detector dead time. This leads to the second constraint, as the need for sufficient statistics requires an equally sufficient experiment time. Luckily, it has been found that even with the minimum available deposit mass, there is for every loading step at least one detector that attains a good amount of statistics in a very reasonable amount of time.

One possible way of improving the feasibility of the experiment would be to circumvent the limited availability of detectors with small deposit masses, the most useful ones for avoiding dead time problems. This could be done by acquiring more of them, or in the case of that not being possible, by repeating the measurements several times, modifying the position of the detectors on each of them to cover all the necessary sites.

To sum up, the present work has shown favorable results, that deem the SALMON phase 2 PNS experiments completely feasible in the conditions that we have studied, for the last steps of the loading process, with the usage of the area method as a reactivity measuring technique. The importance of detector positioning, deposit choice, intrinsic source monitoring, dead time and experiment time management have been established. It is possible that the designed core does not end up being the definitive one used in the eventual experiments, as that one will most likely include a mixture of UOX and MOX. In that case, further simulations will be required to adjust the aforementioned parameters to the optimal ones for new configurations.

The ultimate goal is to be able to detect loading errors, which is still a distant objective, but this study sits a foundation to further research on the matter.

Bibliography

[1] Alexandre Bailly. "Mesure de la réactivité d'un réacteur sous critique à neutrons rapides". PhD thesis. Normandie Université, 2022.

[2] G Bell. "I and Glasstone S". In: *Nuclear reactor theory* (1970).

[3] D.A. Brown et al. "ENDF/B-VIII.0: The 8th Major Release of the Nuclear Reaction Data Library with CIELO-project Cross Sections, New Standards and Thermal Scattering Data". In: *Nuclear Data Sheets* 148 (2018). Special Issue on Nuclear Reaction Data, pp. 1–142. ISSN: 0090-3752. DOI: https://doi.org/10.1016/j.nds.2018.02.001. URL: https://www.sciencedirect.com/science/article/pii/S0090375218300206.

[4] M.B. Chadwick et al. "ENDF/B-VII.1 Nuclear Data for Science and Technology: Cross Sections, Covariances, Fission Product Yields and Decay Data". In: *Nuclear Data Sheets* 112.12 (2011). Special Issue on ENDF/B-VII.1 Library, pp. 2887–2996. ISSN: 0090-3752. DOI: 10.1016/j.nds.2011.11.002. URL: https://www.sciencedirect.com/science/article/pii/S009037521100113X.

[5] TM Chevret et al. "Reactivity measurement of the lead fast subcritical VENUS-F reactor using beam interruption experiments". In: *PHYSOR2014-The Role of Reactor Physics towards a Sustainable Future*. 1087437. 2014, 15–p.

[6] Ministère de la transition Écologique. *Chiffres clés de l'énergie, Édition 2021*. 2021. URL: https://www.statistiques.developpement-durable.gouv.fr/edition-numerique/chiffres-cles-energie-2021/pdf/chiffres-cles-de-l-energie-edition-2021.pdf.

[7] Présentation IDomaines ITextes IRégions. "Doc. Enreg. le &/. j 0 L.." In: ().

[8] Andrew E. Johnson et al. "serpentTools: A Python Package for Expediting Analysis with Serpent". In: *Nuclear Science and Engineering* 194.11 (2020), pp. 1016–1024. DOI: 10.1080/00295639.2020.1723992.

[9] J. R. Lamarsh. *Introduction to Nuclear Reactor Theory*. American Nuclear Society, 1966. ISBN: 978-0-89448-040-9. URL: https://www.ans.org/store/item-300030/.

[10] Jean-Luc Lecouey. "Reactivity Monitoring of Accelerator Driven Subcritical Reactors". HDR memory in Physics, presented on 2019.

[11] JL Lecouey et al. “Reactivity measurement with threshold fission chambers in the MYRRHA mock-up fast subcritical reactor Venus-F”. In: (2018).

[12] Jaakko Leppänen et al. “The Serpent Monte Carlo code: Status, development and applications in 2013”. In: *Annals of Nuclear Energy* 82 (2015). Joint International Conference on Supercomputing in Nuclear Applications and Monte Carlo 2013, SNA + MC 2013. Pluri- and Trans-disciplinarity, Towards New Modeling and Numerical Simulation Paradigms, pp. 142–150. ISSN: 0306-4549. DOI: https://doi.org/10.1016/j.anucene.2014.08.024. URL: https://www.sciencedirect.com/science/article/pii/S0306454914004095.

[13] Nathalie Marie et al. “Reactivity monitoring using the area method for the subcritic al VENUS-F core within the framework of the FREYA Project”. In: *arXiv preprint arXiv:1306.1063* (2013).

[14] William H Press and Saul A Teukolsky. “Savitzky-Golay smoothing filters”. In: *Computers in Physics* 4.6 (1990), pp. 669–672.

[15] Doug Reilly et al. *Passive nondestructive assay of nuclear materials*. Tech. rep. Nuclear Regulatory Commission, Washington, DC (United States). Office of . . ., 1991. Chap. 11.

[16] P Rinard et al. “Neutron interactions with matter”. In: *Passive nondestructive assay of nuclear materials* 375-377 (1991).

[17] J Kenneth Shultis and Richard E Faw. *Fundamentals of Nuclear Science and Engineering Third Edition*. CRC press, 2016.

[18] Aude Verdier. “Evaluation de la sous-criticité lors des opérations de chargement d’un réacteur nucléaire REP”. PhD thesis. Université Claude Bernard-Lyon I, 2005.